

Ternary blend nanofibers of PLA/PCL/CAB for skin tissue scaffolds: Influence of blend ratio and PCL molecular mass on miscibility, morphology, crystallinity and thermal properties

Nantaprapa Tuancharoensri¹ Gareth Ross^{1,2} Sararat Mahasaranon^{1,2} Paul D. Topham³ and Sukunya Ross^{1,2,*}

¹Department of Chemistry, Faculty of Science, Naresuan University, Phitsanulok 65000, Thailand

²Excellent Center of Biomaterials, Department of Chemistry, Faculty of Science, Naresuan University, Phitsanulok 65000, Thailand

³Aston Institute of Materials Research, Aston University, Birmingham, B4 7ET, UK
Phone +55 963 401-2, Fax. +55 963 402, *e-mail: sukunyaj@nu.ac.th

ABSTRACT

Ternary blends of poly(lactic acid) (PLA), polycaprolactone (PCL) and cellulose acetate butyrate (CAB) were fabricated into the form of electrospun nanofibers targeted for skin tissue scaffolds. The effect of blend ratio and molecular mass of PCL (PCL1 and PCL2) on morphology, miscibility, crystallinity, thermal properties, surface hydrophilicity and cell culture of the nanofibers were investigated. Blends with high PLA loading (80/10/10 PLA/PCL/CAB) gave fibers with a smooth surface, owing to the enhanced miscibility between the polymer chains from the presence of CAB, which acts as compatibilizer. In contrast, blends with high PCL loading were immiscible, which led to beads during the electrospinning process. Increasing the molecular mass of PCL2 produced smoother fibers than low molecular mass of PCL1. The XRD patterns of both blends of PLA/PCL1/CAB and PLA/PCL2/CAB gave similar traces to one another, in which the high crystalline peaks of PCL were seen in 20/70/10 blends, were very small in 50/40/10 blends and much less prevalent in the 80/10/10 blends. Better fiber formation (80/10/10 > 50/40/10 > 20/70/10) less crystallinity occurs in well-formed fibers. Selected blends of PLA/PCL/CAB promoted growth of NIH/3T3 fibroblast cells, demonstrating that our novel biocompatible ternary blend nanofibrous scaffolds have the potential in skin tissue repair applications. In addition, this work helps to design and understand the factors that control the properties of nanofibrous scaffolds of PLA/PCL/CAB.

INTRODUCTION

Various types of biocompatible materials from either synthetic or natural routes have been fabricated into the nanofibrous scaffold for skin tissue regeneration. Aliphatic biodegradable polyesters, such as poly(lactic acid) (PLA) [1–5], polycaprolactone (PCL) [1,6], and poly(glycolic acid)s (PGA) [7,8] and their copolymers [8–10], are popular material choices in this field, due to their biocompatibility and biodegradability. PLA, a bio-based polymer derived from sugarcane, potato and corn [11] with great potential, but suffers from inherent brittleness. In order to improve its mechanical properties, PLA has been blended with other bio-based materials, such as PCL [1,12], chitosan [4], PGA [13] and poly(3-hydroxybutyrate-co-3-hydroxyvalerate) (PHBV) [14].

Nanofibers have been extensively used in many fields, for example, electrical and optical applications [15], filtration [16,17], biosensors [18,19], reinforced composites [20,21], and many biomedical applications (e.g. tissue engineering [22,23], drug release [24–26], wound dressings [13] and enzyme immobilization [27]). Nanofibrous scaffolds for skin tissue regeneration have become an important theme in the medical field that can help patients who suffer from chronic wounds, including diabetic foot ulcers and pressure sores. The benefit of nanofibers is they have a similar structure to the extracellular matrix (ECM) with a large surface area that human skin cells can adhere to proliferate on [28], as well as promoting fluid absorption processes [29].

The inherent hydrolytic instability of PLA taken together with the greater stability of PCL provides a family of polyesters systems showing a useful spectrum of stability in which the additional use of phase separated blends can be exploited to influence degradability and the toughness of PLA [30]. Blending techniques have been widely employed to enhance the toughness of PLA by an increase in inter-phase bonding through the use of a further component that acts as a compatibilizer. A key strategy is to combine the characteristic properties of multiple unique polymers to fine-tune the nanofibers to meet the criteria of end-use, instead of relying on the singular attributes of an individual component. Wu and co-workers studied the morphology and orientation of binary blended PLA/PCL nanofibers, created by electrospinning [1]. This work demonstrated that phase separation between PLA and PCL occurs inside the fibers due to their inherent immiscible. Other researchers have characterized nanofibers by studying the effect of morphology, structure, mechanical properties, biodegradability, cell seeding and cell adhesion [31–35].

An important point of note about the work presented is that although electrospun binary blends are considerably represented in the literature; electrospun three component blends have rarely to appear. In addition, detailed studies of morphology, miscibility, crystallinity, thermal properties and fibroblast cell viability of electrospun nanofibers from ternary blends based on PLA have not been previously reported. This is, in part, perhaps a reflection of the fact that rigorous, systematic experimental investigation of three component systems is extremely time consuming. In this paper, ternary blend electrospun nanofibers of PLA, PCL and cellulose acetate butyrate (CAB) have been investigated in an attempt to design new biodegradable tissue cell scaffolds with tunable properties. CAB was chosen because of its known compatibility with ester-containing polymers, provided by the miscibility prediction between polymer pairs developed by Coleman and Painter and our previous researches [30,36,37].

Herein, we report electrospun nanofibers from ternary blends of PLA/PCL/CAB at three different blending ratios of 80/10/10, 50/40/10 and 20/70/10 with PCL of two different molecular masses (PCL1 and PCL2). These blending ratios were selected using optical ternary phase diagrams (showing apparent miscibility or immiscibility) as preliminary guide for the composition selections, the rational for this is described in the section of film formation by the rapid screening method. The nanofibrous scaffolds of PLA/PCL1/CAB and PLA/PCL2/CAB were then compared in terms of physical structure, miscibility, crystallinity, thermal properties and fibroblast cell culture ability to probe their potential for skin tissue scaffolds. This work also usefully compared the characteristics of the fibers and films of PLA/PCL/CAB in terms of crystallinity.

EXPERIMENTAL

Materials

Poly(lactic acid) (PLA) was supplied by PTT Global Chemical Co. Ltd, Thailand ($M_n = 58,800 \text{ g.mol}^{-1}$, 4032D). Two different molecular masses of polycaprolactone (PCL), PCL1 ($M_n = 42,500 \text{ g.mol}^{-1}$) from Sigma-Aldrich Co. Inc. Gillingham, Dorset, UK, and PCL2 ($M_n = 80,000 \text{ g.mol}^{-1}$) from Shenzhen Esun Industrial Co., Ltd, Guangdong, China, were used. Cellulose acetate butyrate (CAB) ($M_n = 30,000 \text{ g.mol}^{-1}$, 2 wt% acetyl and 52 wt% butyryl content) was purchased from Sigma-Aldrich, UK. Chloroform (CF) and dimethylformamide (DMF) were used as solvents for electrospinning, from RCI Labscan Limited, Bangkok, Thailand.

For cell culture studies, mouse fibroblast cell lines (NIH/3T3) purchased from ATCC (American Type Culture Collection, USA) and a medium of Dulbecco's modified eagle's medium (DMEM)/F12 were purchased from Sigma–Aldrich (St. Louis, MO). Fetal bovine serum (FBS) was purchased from Gibco (Grand Island, NY). Trypsin/ethylenediamine-tetraacetic acid (EDTA) (0.25%) were purchased from Gibco (Grand Island, NY). 3-(4,5-dimethylthiazol-2-yl)-2,5-diphenyltetrazolium bromide (MTT); ultra pure grade was supplied by Amresco®, Solon, USA. Dimethylsulfoxide (DMSO); cell culture grade was supplied by Sigma-Aldrich, St. Louis, MO, USA).

Fabrication of electrospun nanofibers

Three different compositions of PLA/PCL1/CAB and PLA/PCL2/CAB (80/10/10, 50/40/10 and 20/70/10) were selected for fiber fabrication *via* electrospinning. The sample compositions were selected based on high, medium and low loadings of PLA and PCL with a constant loading of CAB at 10 wt%, which acts as a compatibilizer in the system. These compositions selected also corresponded to different regions in optical clarity of solvent blended films from the optical ternary phase diagrams (showing apparent miscibility or immiscibility) that were constructed by the rapid screening method (see Figure 7). A simple and inexpensive electrospinning apparatus was set up to produce continuous fibers. A high-voltage power supply (maximum voltage 30 kV, Genvolt, General High Voltage Ind. Ltd, UK), a precision pump (NE-300, New Era Pump Systems, Inc., USA) and a grounded aluminum foil collector were used as supplied.

All homopolymer solutions were prepared at a concentration of 10 %w/v in 4:1 (w/w) using CF/DMF, and then mixed in the appropriate proportions to give the desired ternary polymer blend solutions. CF is a good solvent for all polymers used in this study with a dielectric constant of 4.8 at 20 °C, while DMF was chosen to enhance the conductivity of the polymer solution for electrospinning, as it possesses a high dielectric constant of 38.3. The solutions were then loaded in a typical plastic medical syringe with metal needle (internal diameter of 0.7 mm) and the needle was attached to the high voltage supply. Optimum conditions were found to be: flow rate of 0.5 mL/h, applied voltage of 25 kV and tip-to-collector distance of 10 cm. Electrospun nanofibers were collected on an aluminum foil collector and dried at room temperature as nonwoven fibers.

Rapid screening method for construction of optical ternary phase diagram

Ternary blends (PLA/PCL/CAB) with different PCL molecular masses were prepared using the rapid screening method. This combinatorial technique, described previously, uses transmission spectrophotometry, a 96-well plate and a multi-wavelength plate reader, which enables a large number of samples to be measured quickly [30]. Consequently, one can rapidly produce an optical ternary phase diagram in order to predict apparent miscibility by using optical clarity of the solvent blended films. Briefly, individual polymers were dissolved in CF at 10 wt% and then pipetted into a 96-well plate at various compositions. The solvent in the sample was then evaporated slowly for 24 hours to allow equilibrium morphology to be attained. Transmittance (%T) of the blended films at wavelength 450 nm was measured using a microplate reader. Films are defined as clear (apparent miscible) when %T \geq 76, translucent at %T = 51-75, semi-translucent at %T = 31-50 and opaque (immiscible) at %T = 0-30. Figure 7 shows the optical ternary phase diagrams of PLA/PCL1/CAB and PLA/PCL2/CAB.

Characterization of electrospun nanofibers

Morphology: The morphology of ternary blend nanofibers was observed by scanning electron microscopy (SEM, Leo Model 1455VP) at 20 kV in high vacuum. Samples were cut into squares of 0.5 x 0.5 mm before being mounted on to metal stubs and deposited with gold to enhance the electrically conductive property. Different areas of the sample surfaces were investigated and recorded at different magnifications.

Miscibility: Miscibility of ternary blend nanofibers was observed by Attenuated Total Reflectance-Fourier Transform Infrared Spectroscopy (ATR-FTIR), Perkin Elmer Spectrum GX, 4000-400 cm^{-1}).

Crystallinity: Crystallinity of ternary blend nanofibers was investigated by X-Ray diffraction (XRD, Philips Model X'Pert Pro) with a diffraction angle range (2θ) from 5 to 60 degrees ($\lambda = 1.54 \text{ \AA}$).

Thermal properties: Thermal properties were investigated by differential scanning calorimetry (DSC, Mettler Model DAC1). Ternary blend nanofibers were heated from 25 to 200 °C (first heat), cooled to -100 °C and then heated to 200 °C (second heat) at heating and cooling rates of 10 °C/min under a nitrogen atmosphere.

Hydrophilicity: Hydrophilicity of ternary blend nanofibers was measured by static contact angle (CA, Dataphysics Model OCA20) using distilled water at room temperature.

Cell culture studies of ternary blend nanofiber scaffolds

Cell culture preparation: Mouse fibroblast cell lines (NIH/3T3) were cultured in a flask with DMEM-F12 medium supplemented with 10% FBS and 1% Pen/step and maintained at 37 °C under 5% CO₂ humidified atmosphere. The culture medium was refreshed every 2-3 days.

Sterilized scaffolds: Ternary blend scaffolds of PLA/PCL1/CAB and PLA/PCL2/CAB at different compositions were cut to a size of 5 x 5 x 0.7 mm and added into the 96-wells plate. The scaffolds were sterilized with ethanol under UV light for 30 mins and washed with PBS solution.

Cell seeding: The sterilized scaffolds were soaked in the culture medium (90 DMEM:10 FBS) for 1 hour and then left for another hour in a closed system (incubator at 37 °C). Finally, mouse fibroblast cell line (5×10^5 cells) was seeded on each scaffold for cell proliferation studies. Tissues culture polystyrene plates (TCPS) were used as a control.

Cell proliferation: MTT assay: The proliferation of cells on the scaffold were studied after 3 and 6 days of culture using an MTT assay. MTT was added to the medium containing cell-loaded scaffolds and left for 4 hours in an incubator before removal of the medium. Cultured scaffolds were put into vials and then 200 μ L of DMSO:ethanol (EtOH) (1:1 v/v) was added, put into an ultrasonic bath for 30 mins and left overnight before measuring the optical density (OD) by UV-Visible spectrophotometry, using a microplate reader at 590 nm (where the measured absorbance is directly related to the number of proliferated cells). The active mitochondria of the viable cells reduce the yellow coloured of MTT into blue formazan crystals, which indicates cellular viability. Scaffolds with no cells as well as the controlled sample (cells with no scaffold) were also measured and the OD value of scaffolds with no cells loading were subtracted from the OD values of all loaded scaffolds [38].

RESULTS AND DISCUSSION

There are many factors that influence the internal molecular structure and properties of electrospun nanofibers (*i.e.* flow rate of polymer solution, applied voltage, tip-to-collector distance, ambient parameters, polymer solution concentration, polymer molecular mass, viscosity, surface tension and conductivity), which in turn govern the end-use of the nanofibers [39,40]. Consequently, the effect of blend ratio and PCL molecular mass (PCL1 and PCL2) on morphology, miscibility, crystallinity, thermal properties, hydrophobicity and cell culture ability of the ternary blend electrospun nanofibers were studied. The number-

average molecular mass of PCL2 was approximately twice that of PCL1 (PCL1, $M_n = 42,500$ g.mol⁻¹ and PCL2, $M_n = 80,000$ g.mol⁻¹).

The electrospinning processing conditions were studied and optimized to the most suitable parameters for PLA/PCL/CAB blends, which were used for all subsequent tests (applied voltage 25 kV, polymer concentration 10 wt% in 4:1 CF/DMF, flow rate 0.5 mL/h and a tip-to-collector distance of 10 cm). Humidity and temperature are shown to effect fiber formation [41]. During these experiments the humidity and temperature did not significantly change and were in the range of ~50-60% humidity and 27-28 °C, respectively. To understand the advantage of using ternary blends, the properties of the homopolymers (PLA, PCL1, PCL2 and CAB) and PLA/PCL blend were also studied.

Morphology of homopolymers and PLA/PCL

The electrospun fibers of homopolymers (PLA, PCL1, PCL2 and CAB) and binary blend of PLA/PCL were fabricated using the electrospinning parameters for PLA/PCL/CAB blends and their morphology studied by SEM. The use of the same electrospinning parameters as ternary blends are not the ideal parameters for each homopolymer but selected to allow for better understanding of the results obtained for the ternary blend nanofibers. Figure 1 shows the SEM images of electrospun samples at a concentration of 10 w/v% for PLA, PCL1, PCL2 and CAB, and 50/50 PLA/PCL2.

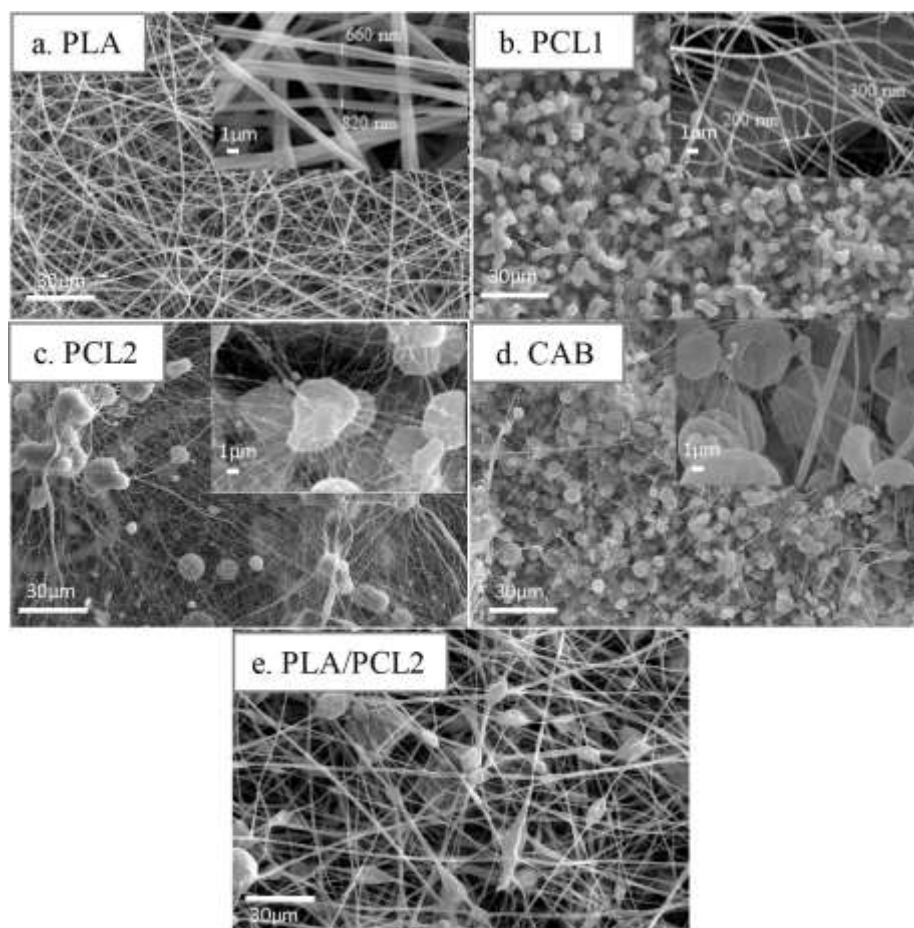


Figure 1. SEM images of electrospun samples at a concentration of 10 w/v% for PLA, PCL1, PCL2 and CAB, and 50/50 PLA/PCL2.

PLA was successfully fabricated into bead-less fibers with a smooth surface with diameters in the range of 660-820 nm. The images of PCL1, PCL2 and CAB show ultrafine fibers with diameters in range of 100-300 nm with a high proportion of beads. In case of the formation of beads of PCL1, PCL2 and CAB, it is possibly caused by using low concentrations of their solutions or low molecular weight, which produces a low degree of chain entanglement. PCL2 has two times higher in molecular weight than PCL1, which can produce higher chain entanglements and intermolecular interactions resulting to form less numbers of beads and provides more interchain connectivity. In addition, a binary blend of PLA/PCL2 was also investigated. This 50/50 blend formed undulating fibers with a high number of beads. In summary, the homopolymer fibers fabricated using the same controlled parameters found that PLA formed well-define fibers, while the use of higher molecular weight PCL2 formed smoother fibers with less beads than PCL1 and CAB formed mainly beads with very fine diameter fibers.

Morphology of ternary blend nanofibers of PLA/PCL1/CAB and PLA/PCL2/CAB

Figure 2 shows SEM images of the electrospinning nonwoven fibers of two different ternary blends (PLA/PCL1/CAB and PLA/PCL2/CAB) at three different compositions (80/10/10, 50/40/10 and 20/70/10) at a total polymer concentration of 10 wt% and 4:1 w/w CF:DMF.

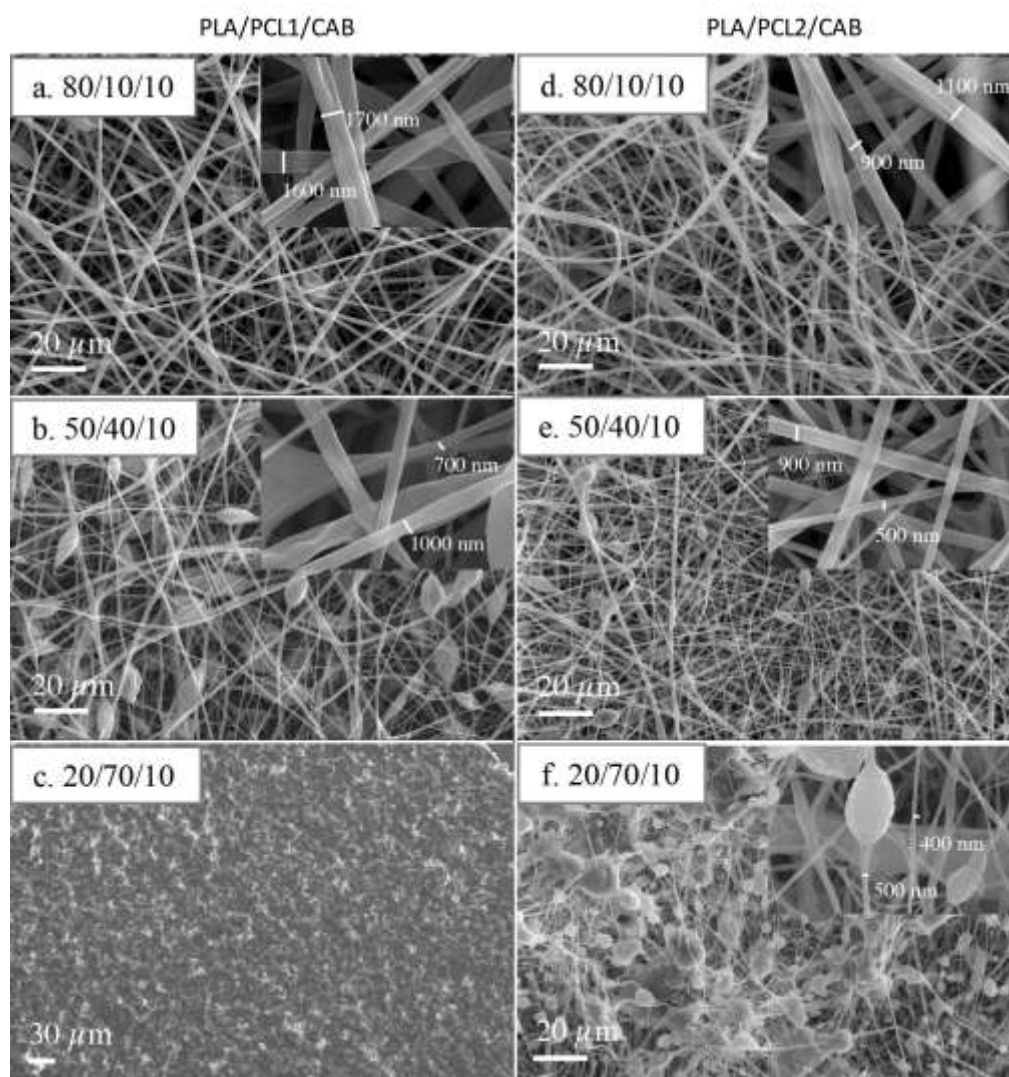


Figure 2. SEM images of ternary blend electrospun nanofibers of PLA/PCL1/CAB (a, b, c) and PLA/PCL2/CAB (d, e, f) at different compositions.

Comparing the fibers fabricated from PLA/PCL1/CAB at different compositions (with the CAB content kept constant), the ternary blend fibers at 80/10/10 have diameters in the range of 1.6 – 1.7 μm, with smooth surfaces and a small number of beads (Figure 2a).

The 50/40/10 blend produced fibers mixed with beads with fiber diameters in the range of 700 nm–1 μ m (Figure 2b). Finally, in the blend of 20/70/10 PLA/PCL1/CAB (Figure 2c), no fibers were formed under the same conditions.

These findings indicate the effect of ternary blend composition on the fiber morphologies. With increasing PCL1 content, the ability to create smooth and continuous nanofibers is reduced; bead density increased with a concomitant decrease in average diameter of the fibers, until no fibers could be formed (at highest PCL1 loadings). Noticeably, using high loading of PLA encourages the formation of more uniform fibers. This is due to increased PLA chain entanglement compared to PCL1, which results in longer continuous fibers as the continuity of the polymer solution jet is elongated. In addition, the average fiber diameter increases as the PLA content increases due to greater resistance to stretching and elongation of the higher PLA solution viscosity.

After studying the fabrication of PLA/PCL1/CAB fibers, higher molecular mass PCL was used in the ternary blend (PLA/PCL2/CAB) in an attempt to increase entanglements to fabricate smoother fibers (with less beads). Figure 2 shows that PLA/PCL2/CAB produced less beads than PLA/PCL1/CAB at the same blend compositions, as expected. Beaded electrospun fibers are common and their formation usually occurs due to the concentration of the solution or molecular weight of the polymer being too low. Experiments have shown that the main influences that lead to bead formation are low molecular weight, concentration, viscosity, high surface tension and low charge density [42]. The mechanism is due to Rayleigh instability driven by surface tension, in that the fluid jet will minimize the surface area. If the viscoelastic force of the jet can oppose this instability, then a smooth fiber will form [43]. This is completely in line with the results obtained herein, with PCL2 providing more entanglements and thus better viscoelastic performance.

For both ternary blends (using PCL1 or PCL2), more beads were formed when higher PCL contents were used, which corresponds to the results seen with the homopolymers and binary blends. Interestingly, whilst the PCL1-based ternary blend with high PCL content (20/70/10) gave no fibers, the PCL2-based equivalent produced fibers, but with a high amount of beads. It is therefore noteworthy that the morphology of the fibers (diameter, surface topography, beads) depends not only on the blend composition, but also on the molecular mass of the materials used, as discussed elsewhere [40].

Miscibility studies of ternary blend nanofibers of PLA/PCL1/CAB and PLA/PCL2/CAB

PLA and PCL are immiscible and, hence, will form a typical two-phase system in their blends (if provided with sufficient mobility) [1]. This is also likely to occur in ternary blends containing these polymers if the third component does not have a sufficiently high compatibilizing effect or if there is simply not enough of the third component. However, the presence of PCL is known to enhance the toughness of PLA and increase the biodegradable time of such blends, which can be an advantage for tissue engineering scaffolds that can benefit from the biocompatibility, biodegradability, minimal inflammatory reaction and excellent mechanical properties of PCL [1,44].

Herein, CAB has been chosen as a third component to act as a compatibilizer between PLA and PCL because of its known compatibility with ester-containing polymers, and could promote the miscibility of ternary blends of PLA/PCL/CAB. The miscibility or immiscibility of ternary blend fibers can be observed using FTIR spectroscopy. If the blends are immiscible, the FTIR spectrum of the blends is simply the summation of the spectra of the two or three homopolymers, while shifts in the characteristic bands in the FTIR spectrum describes indicates a level of miscibility [30,37,45]. Figure 3 shows the FTIR spectra of electrospun fibers of the homopolymers (PLA, PCL, CAB) and the blends. *N.B.* The FTIR spectra of PCL1 and PCL2 are identical and have therefore been shown as PCL to represent both PCL1 and PCL2.

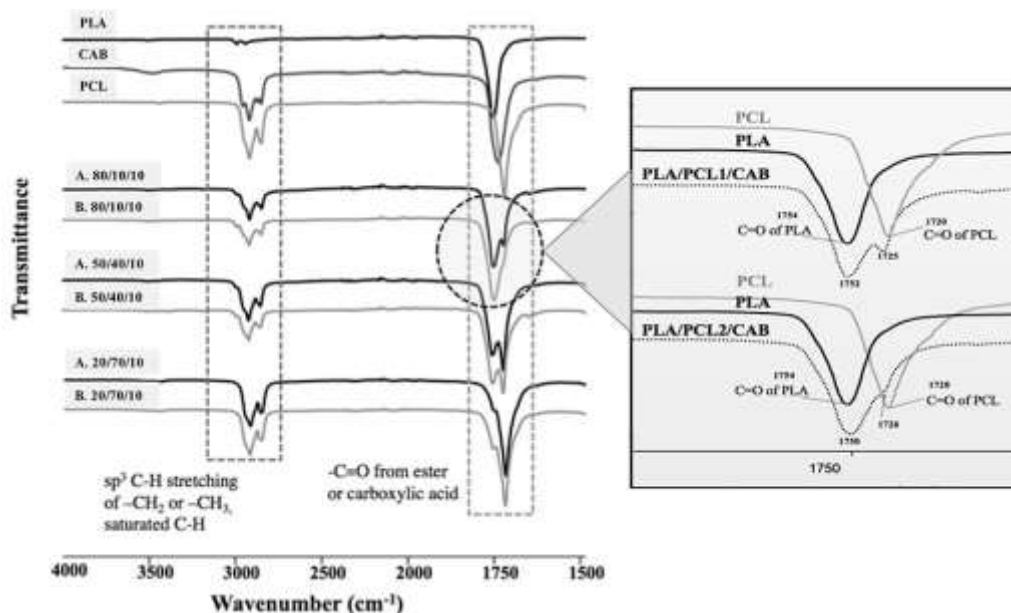


Figure 3. FTIR spectra of nonwoven ternary blend nanofibers of: (A) PLLA/PCL1/CAB and (B) PLLA/PCL2/CAB, at different compositions.

PLA, PCL and CAB homopolymer fibers show FTIR absorption bands of sp^3 C-H stretching of $-CH_2$ or $-CH_3$ or saturated $-CH$ at $2700-2800\text{ cm}^{-1}$, and bands of $-C=O$ from ester or carboxylic acid groups at $1730-1750\text{ cm}^{-1}$. All of these spectra are similar but show a small difference in their band positions. For example, the $-C=O$ peak of PLA is observed at 1754 cm^{-1} , while those of CAB and PCL are at 1738 cm^{-1} and 1720 cm^{-1} , respectively. The FTIR spectra of 50/40/10 and 20/70/10 of both PLA/PCL1/CAB (A) and PLA/PCL2/CAB (B) are simply the spectrum sum of the homopolymers, indicating that they are likely to be immiscible blends. The carbonyl stretching vibration region of the blends at high PLA loading (80/10/10) appears to be shifted from the homopolymers, in which the carbonyl band of PLA is shifted to a lower frequency (loose intermolecular packing indicating a freedom of movement), PCL is shifted to a higher frequency (close intermolecular packing indicating self-aggregation) and the CAB carbonyl band cannot be seen. Additionally, the carbonyl band is broader, particularly for the PLA/PCL2/CAB blend. This confirms that the blends of PLA/PCL1/CAB and PLA/PCL2/CAB at high PLA loading show similar behavior in terms of blend miscibility and the blend seems to be more miscible when using high molecular mass PCL2. The blends with higher PCL loading (50/40/10 and 20/70/10) appear to be more immiscible.

Crystallinity of ternary blend nanofibers of PLA/PCL1/CAB and PLA/PCL2/CAB

Figure 4 shows the XRD patterns of homopolymer fibers and nonwoven ternary blend nanofibers of PLA/PCL1/CAB (A) and PLA/PCL2/CAB (B). Homopolymer fibers of PCL (representing both PCL1 and PCL2) exhibited two main diffraction peaks at 2θ values of 21.5° and 24° , while PLA and CAB have no observable crystalline peaks, only broad peaks from the amorphous phases. Electrospinning provides a quench process for the polymer solution, where the solvent evaporates rapidly. Therefore, the polymer chains have much less time to self-organize and crystallize, producing more amorphous regions in the electrospun fibers. As seen, PLA, a semi-crystalline polymer, is the only polymer that formed solely fibers (see Figure 1.) and no crystalline peaks were observed in the XRD pattern. Whereas, PCL (a semi-crystalline polymer) formed beads during electrospinning and crystalline peaks were observed. The possible reason is that PCL crystallizes more easily than PLA, which is determined by nature of two polymers. In addition, the solvent is removed more slowly from

the aggregated beads of PCL, which allows more time for the polymer chains to align and adopt more crystalline domains. Although beads were produced during the electrospinning process of CAB, no crystalline peaks were observed in the XRD pattern because CAB is an amorphous polymer.

The XRD patterns of both blends of PLA/PCL1/CAB and PLA/PCL2/CAB gave similar traces to one another, in which the high crystalline peaks of PCL were seen in 20/70/10 blends, were very small in 50/40/10 blends and much less prevalent in the 80/10/10 blends. These results correspond to the observations from the SEM images of the ternary blends in Figure 2, with better fiber formation following the trend of 80/10/10 > 50/40/10 > 20/70/10 *i.e.* less crystallinity occurs in well-formed fibers.

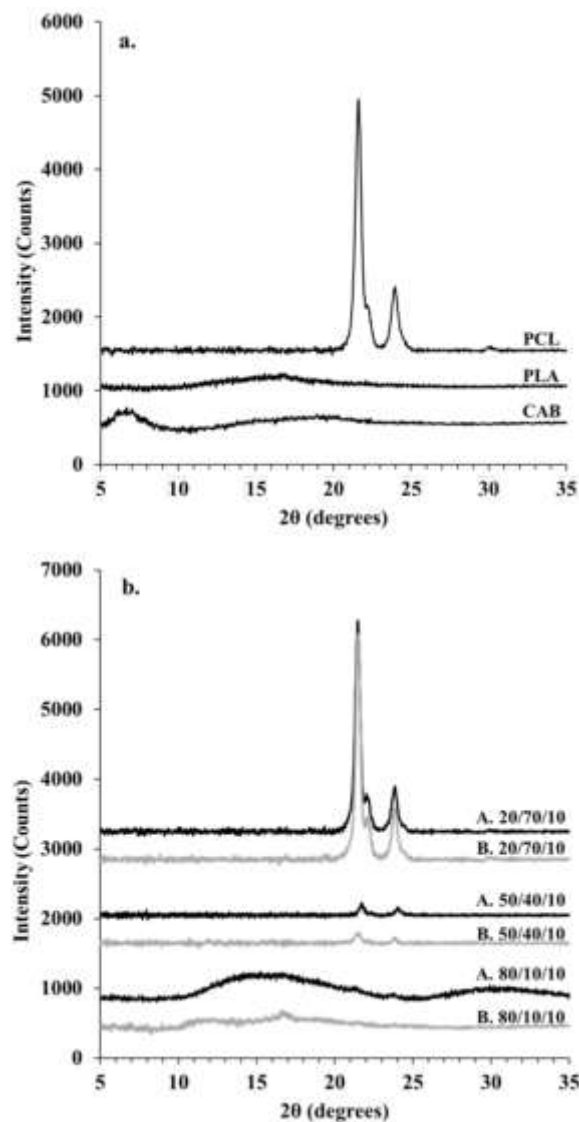


Figure 4. XRD patterns of homopolymer fibers and ternary blend fibers; PLLA/PCL1/CAB (A.) and PLLA/PCL2/CAB (B.) at different compositions.

Thermal properties of ternary blend nanofibers of PLA/PCL1/CAB and PLA/PCL2/CAB

Figure 5 shows the DSC thermograms of the first heating, cooling and second heating runs of the non-woven ternary blend nanofibers of PLA/PCL1/CAB and PLA/PCL2/CAB blends at different compositions. These data sets demonstrate that the crystallization temperature (T_c) of PCL (both PCL1 and PCL2, see Fig. 5b) was dependent on blend composition, in which the T_c peak of PCL shifted towards a lower temperature and size of the crystallization exothermic peaks decreased with a decrease in PCL content. In addition, the T_c peak of PCL2 in PLA/PCL2/CAB blends (dashed line) shifted towards a lower temperature than the T_c peak of PCL1 in the PLA/PCL1/CAB blends (solid line). For the first and second heating runs for both blends (Fig. 5a and 5c), it can be seen that the melting temperature (T_m) of PCL (ca. 55 °C) and that of PLA (ca. 167 °C) do not significantly change in all compositions. The cold crystallization temperature (T_{cc}) peak of PLA are observed in the second heating run (Fig. 5c), with the position shifted towards a lower temperature when PCL2 was incorporated in the blends because of enhanced opportunity for alignment of the longer chains.

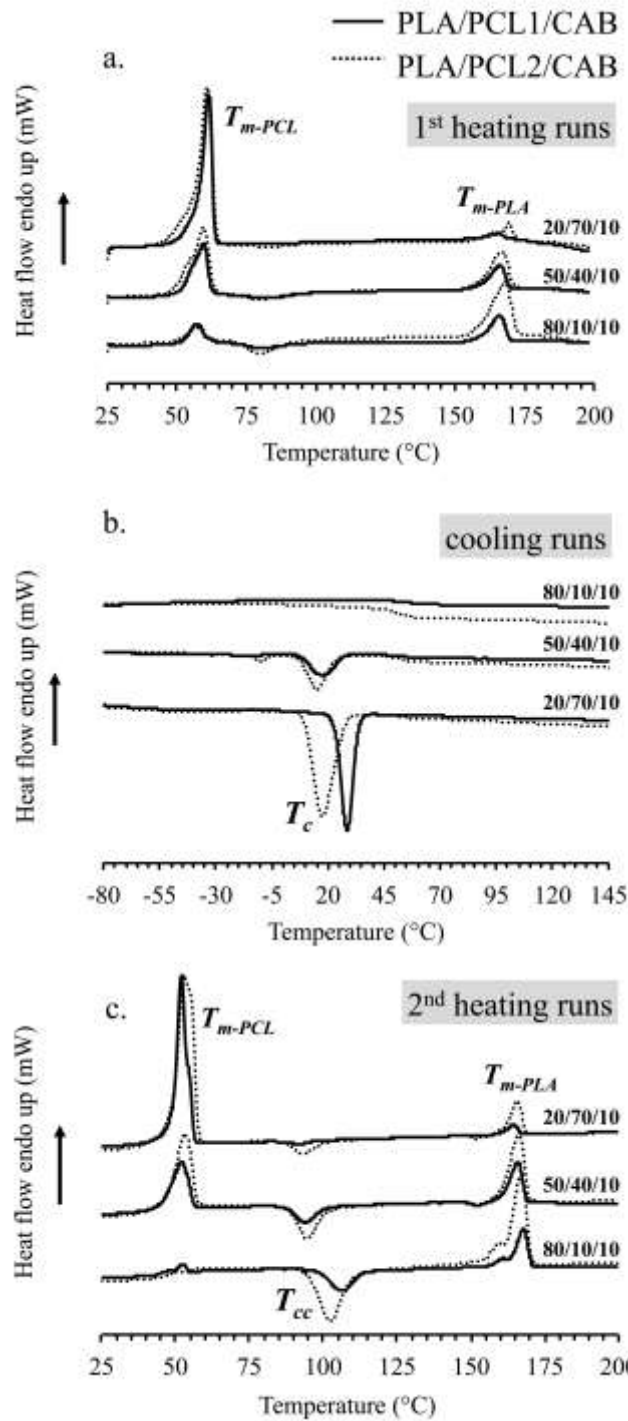


Figure 5. DSC thermogram of non-woven ternary blend fibers; a. at 1st heating runs, b. at cooling runs and c. at 2nd heating runs, of PLA/PCL1/CAB and PLA/PCL2/CAB.

Cell proliferation: MTT assay of ternary blend nanofibers of PLA/PCL1/CAB and PLA/PCL2/CAB

Prior to cell studies, contact angle measurements were performed on the fibrous scaffolds to ascertain the hydrophilic character of the blends as this property help promote the

adhesion of skin cells. The hydrophilicity of the ternary blend nanofibers were in the range of 130-140°, which were similar or slightly higher than homopolymer fibers alone. The homopolymer fibers of PLA, PCL and CAB had contact angles of 137°, 97° and 133°, respectively. The blends that were able to form electrospun nanofibrous constructs (*i.e.* PLA/PCL1/CAB and PLA/PCL2/CAB at 80/10/10 and 50/40/10) were selected for cell culture studies. Proliferation of cells loaded on these ternary blend scaffolds was studied by MTT assay for 3 days and 6 days and the results are shown in Figure 6. It can be seen that the growth of NIH/3T3 fibroblast cells in the control polystyrene plate confirmed the viability of the cells. For PLA/PCL1/CAB scaffolds, cell growth or proliferation was better when they were cultured on 80/10/10 blend scaffolds than on 50/40/10 blend scaffolds. This is attributed to the better morphology of the 80/10/10 fibers (Figure 2a), compared to 50/40/10 fibers (Figure 2b) that contains beads, which creates an uneven platform with lower surface area for cells to grow. Comparing the same blend compositions of PLA/PCL1/CAB scaffolds, the cell viability slightly increased from day 3 to day 6.

For PLA/PCL2/CAB scaffolds, cell proliferation of both compositions was not significantly different, as the fibers have similar morphologies (Figure 2d and 2e). Finally, the comparison between the blends of PCL1 and PCL2, showed that they both promote cell proliferation similarly. Only the 50/40/10 PLA/PCL1/CAB scaffold showed the lowest cell viability at day 3 due to its beaded structure, as aforementioned. However, its cell viability increased after 6 days of culture. These data suggest that the ternary blend electrospun nanofibrous scaffolds of PLA/PCL1/CAB and PLA/PCL2/CAB at both compositions of 80/10/10 and 50/40/10 promote fibroblast cells growth with the key parameter being the fiber morphology. Even though these two blends are able to promote cell growth, the blend composition is important to fine-tune important properties such as crystallinity, miscibility, thermal properties, hydrophilicity, mechanical strength and degradability.

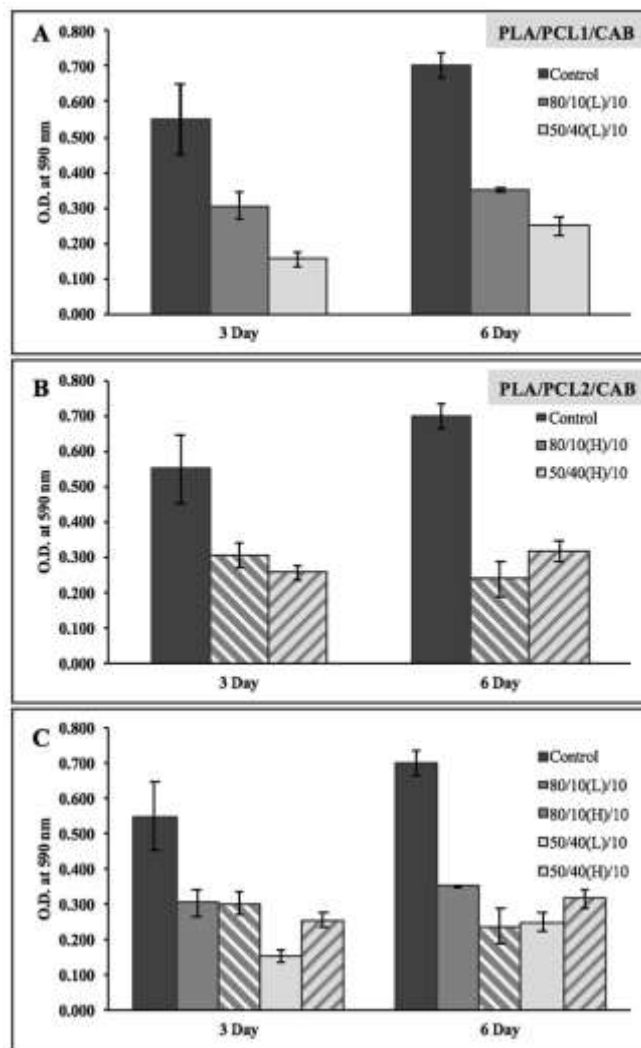


Figure 6. MTT assay showing cell proliferation on the PLA/PCL/CAB scaffolds at different blending ratios after 3 and 6 days of culture; (A) PLA/PCL1/CAB scaffolds, (B) PLA/PCL2/CAB scaffolds, (C) PLA/PCL1/CAB and PLA/PCL2/CAB scaffolds.

Optical ternary phase diagrams and the difference in crystallinity of ternary blend films and electrospun fibers of PLA/PCL/CAB

As previously mentioned, the three different compositions to fabricate electrospun ternary nanofibers were selected from the optical ternary phase diagram constructed by the rapid screening method. In this section, details of the construction of optical ternary phase diagrams and the difference in crystallinity of ternary blend electrospun fibers and ternary solvent blended films of PLA/PCL1/CAB and PLA/PCL2/CAB are described.

Electrospinning provides a quench process for fabricating the polymers into fibers, where the solvent evaporates rapidly and effectively vitrifies the polymer chains far from

equilibrium with a more amorphous structure than would be predicted based on thermodynamic principles. To demonstrate this concept in more detail for our novel blends, whilst highlighting the importance of the processing technique employed, our ternary blends have been cast into films and their phase behavior studied over a wide range of compositions. Importantly, the film formation process used provides an annealing process for the polymers where the solvent evaporates slowly and thus polymer chains have sufficient mobility to demix (phase separate) or intermingle (to homogeneity), depending on the difference in interaction parameters. A rapid screening method, described in our previous work [30], was used to access a large number of blend compositions to create an optical ternary phase diagram for each system. Figure 7 shows the optical ternary phase diagrams of PLA/PCL1/CAB and PLA/PCL2/CAB blends at various compositions.

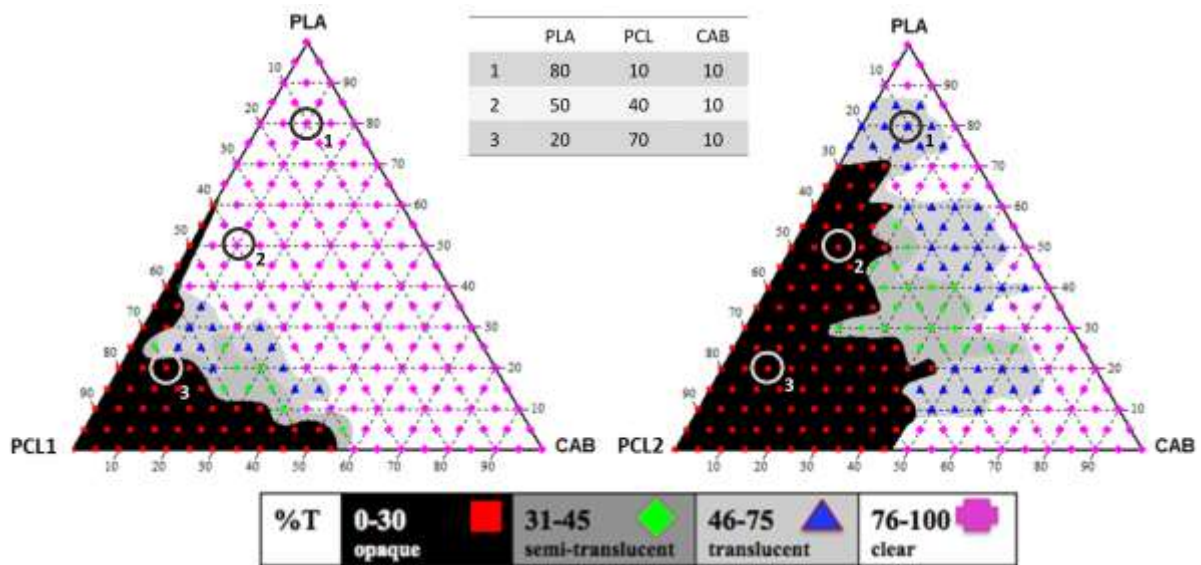


Figure 7. The optical ternary phase diagrams of: PLA/PCL1/CAB (left) and PLA/PCL2/CAB (right) blends; all of the points in the diagrams represent the experimental data to classify the phase regions. *N.B.* The inset table and the circles in the phase diagrams represent the same blend compositions that were used in the electrospinning studies.

The optical ternary phase diagrams were different depending on the PCL molecular mass. High molecular mass PCL2 promotes more opaque regions in the PLA/PCL2/CAB blends. This is attributed to the longer chains of PCL2 promoting alignment of the carbon-carbon backbone. Conversely, the shorter PCL1 is able to intermingle with the other components more readily, restricting alignment of its backbone, resulting in the PLA/PCL1/CAB blend showing more optically clear regions than observed in

PLA/PCL2/CAB. The characteristic properties of films and fibers have been compared at the selected compositions of 80/10/10, 50/40/10 and 20/70/10, as shown in Table 1.

Table 1. Characteristic properties of films and fibers of PLA/PCL/CAB blends at three different blend ratios.

Blends	Film transparency from ternary phase diagrams (Fig. 7*)	Non-woven electrospun fibers from SEM images (Fig. 2)
PLA/PCL1/CAB		
80/10/10	Clear – apparent miscible	Smooth fibers, 1600-1700 nm diameter (some beads)
50/40/10	Clear – apparent miscible	Fiber (700-1000 nm) with beads
20/70/10	Opaque - immiscible	Beads
PLA/PCL2/CAB		
80/10/10	Translucent – partial miscible	Smooth fibers, 900-1100 nm, with no beads
50/40/10	Opaque – immiscible	Fibers, 500-900 nm, with small number of beads
20/70/10	Opaque - immiscible	Fibers with a large number of beads

* It should be noted that the optical transmittance of the films only provide an indication of apparent miscibility, rather than true thermodynamic miscibility.

These different processes, film formation (*via* solvent annealing) and electrospinning (quench), caused the differences in the properties of the final material. The crystallinity of the films was measured at the same compositions used in the electrospinning studies of 80/10/10, 50/40/10 and 20/70/10 and the results are shown in Figure 8. Crystalline peaks of both PLA and PCL were observed in the ternary blends films at intensities much higher than that of electrospun fibers (see Figure 4), as the polymer chains had sufficient mobility to crystallize during film formation.

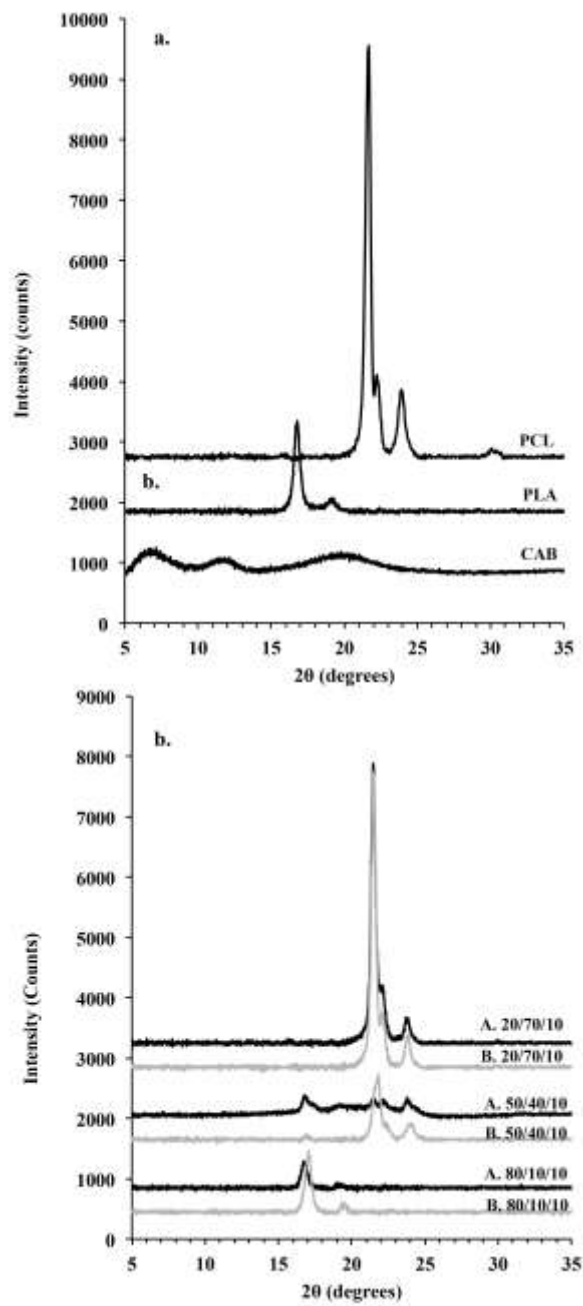


Figure 8. XRD patterns of a. homopolymer films and b. ternary blend fibers; PLLA/PCL1/CAB (A.) and PLLA/PCL2/CAB (B.) at different compositions.

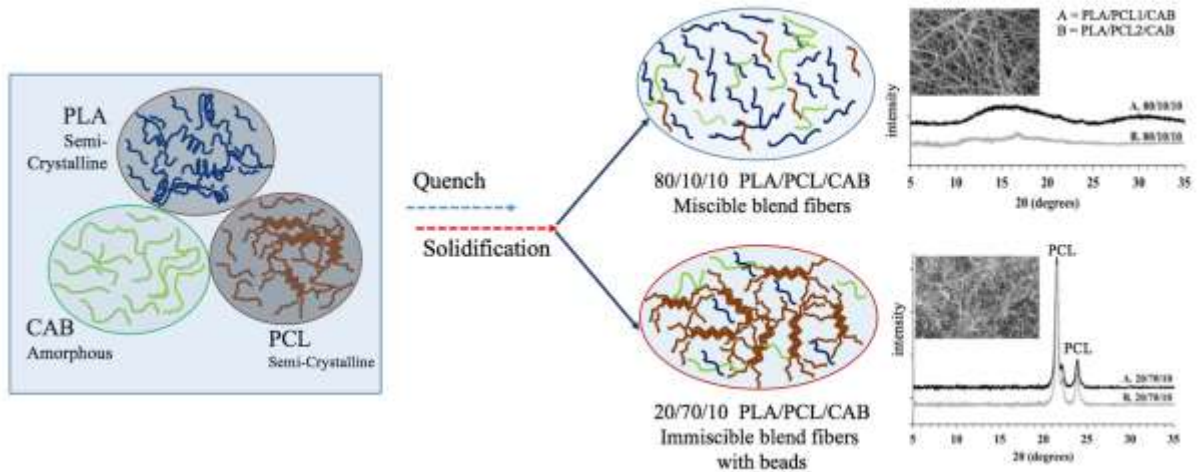


Figure 9. Schematic illustration of the work.

CONCLUSIONS

In this work, ternary blend nanofibrous scaffolds of polyesters, PLA/PCL/CAB, have been successfully prepared by electrospinning and used as tissue cell scaffolds for the first time. PLA and PCL are biodegradable semi-crystalline polymers that are immiscible with one another, therefore CAB was chosen as a third component to act as a compatibilizer (see Figure 9.). Different blend compositions and different PCL molecular masses (PCL1 and PCL2) were selected to process the blends into fibers in order to control the final properties of electrospun nanofiber scaffolds for cell culture studies. The blends at 80/10/10 (PLA/PCL/CAB) with both PCL1 and PCL2 formed smooth fibers with a small amount of PLA crystals, but no crystalline PCL, independent of PCL molecular mass. Interesting, at high PCL loading, the blend at 20/70/10 PLA/PCL1/CAB did not produce fibers (bead formation only), while that of PLA/PCL2/CAB produced ultrafine fibers, but with a large quantity of beads. Our novel polyester blends, at 80/10/10 and 50/40/10 (PLA/PCL/CAB) were studied using MTT assay of NIH/3T3 fibroblast cells and the results showed that these biodegradable scaffolds have potential to be used for skin tissue regeneration.

Acknowledgements

The authors thank to the Annual Government Statement of Expenditure (2014-2015) of Thailand, research number 148525 for the financial support and also thanks to Faculty of Science, Naresuan University for funding this project and Science Lab Centre, Faculty of

Science, Naresuan University for supporting XRD, DSC, SEM, contact angle and FTIR measurement. PDT acknowledges the Royal Society of Chemistry (RSC) (Journal Grant for International Authors) for supporting travel part of this collaborate work.

References:

- [1] Lu L, Wu D, Zhang M and Zhou W, *Ind Eng Chem Res* **51(9)**: 3682-3691 (2012).
- [2] Kim K, Yu M, Zong X, Chiu J, Fang D, Seo Y, Hsiao BS, Chu BM and Hadjiargyrou M, *Biomaterials* **24(27)**: 4977-4985 (2003).
- [3] Ravichandran R, Venugopal JR, Sundarrajan S, Mukherjee S, Sridhar R and Ramakrishna S, *Mater Sci Eng C* **32(6)**: 1443-1451 (2012).
- [4] Cui W, Cheng L, Li H, Zhou Y, Zhang Y and Chang J, *Polymer* **53(11)**: 2298-2305 (2012).
- [5] Thakur RA, Florek CA, Kohn J and Michniak BB, *Int J Pharm* **364(1)**: 87-93 (2008).
- [6] Lowery JL, Datta N and Rutledge GC, *Biomaterials* **31(3)**: 491-504 (2010).
- [7] Park KE, Kang HK, Lee SJ, Min BM and Park WH, *Biomacromolecules* **7(2)**: 635-643 (2006).
- [8] Blackwood KA, McKean R, Canton I, Freeman CO, Franklin KL, Cole D, Brook I, Farthing P, Rimmer S, Haycock JW, Ryan AJ and MacNeil S, *Biomaterials*, **29(21)**: 3091-3104 (2008).
- [9] Bhaarathy V, Venugopal J, Gandhimathi C, Ponpandian N, Mangalaraj D and Ramakrishna S, *Mater Sci Eng C* **44**: 268-277 (2014).
- [10] Ng KW, Khor HL and Hutmacher DW, *Biomaterials* **25(14)**: 2807-2818 (2004).
- [11] Ross GM, Ross S and Tighe BJ, Bioplastics: New Routes, New Products, in *Brydson's Plastics Materials*, 8th ed. by Gilbert M. Elsevier Ltd, Oxford, UK, pp. 631-652 (2017).
- [12] Oliveira JE, Mattoso LHC, Orts WJ and Medeiros ES, *Adv Mater Sci Eng* **2013**: 14 pages (2013).
- [13] Agarwal S, Wendorff JH and Greiner A, *Polymer* **49(26)**: 5603-5621 (2008).
- [14] Li L, Huang W, Wang B, Wei W, Gu Q and Chen P, *Polymer* **68**: 183-194 (2015).
- [15] Luzio A, Canesi EV, Bertarelli C and Caironi M, *Materials*, **7(2)**: 906-947 (2014).
- [16] Sundarrajan S, Tan KL, Lim SH and Ramakrishna S, *Procedia Eng* **75**: 159-163 (2014)
- [17] Graham K, Ouyang M, Raether T, Grafe T, Mcdonald B and Knauf P, The fifteenth Annual Technical Conference & Expo of the American Filtration & Separations Society, Galveston, Texas, USA, April 9-12, 2002.
- [18] Marx S, Jose MV, Andersen JD and Russell AJ, *Biosens Bioelectron*, **26(6)**: 2981-2986 (2011).
- [19] Scampicchio M, Bulbarello A, Arecchi A and Cosio MS, Benedetti S and Mannino S, *Electroanalysis* **24(4)**: 719-725 (2012).
- [20] Xu LR, Li L, Lukehart CM and Kuai H, *J Nanosci Nanotechnol* **7(7)**: 2546-2548 (2007).
- [21] Lin S, Cai Q, Ji J, Sui G, Yu Y, Yang X, Ma Q, Wei Y and Deng X, *Compos Sci Technol* **68(15-16)**: 3322-3329 (2008).
- [22] Vasita R and Katti DS, *Inter J Nanomed* **1(1)**: 15-30 (2006).
- [23] Pham QP, Sharma U and Mikos AG, *Tissue Eng* **12(5)**: 1197-211 (2006).

- [24] Wang L, Wang M, Topham PD and De YH, *RSC Adv*, **2**: 2433-2438 (2012).
- [25] Sill TJ, von Recum HA, *Biomaterials* **29(13)**: 1989–2006 (2008).
- [26] Wei Q and Wei A, Functional nanofibers for drug delivery applications, in *Functional Nanofibers and their Applications*, ed. By Wei Q. Woodhead Publishing Ltd., Cambridge, UK, pp. 153-170 (2012).
- [27] Wang ZG, Wan LS, Liu ZM, Huang XJ and Xu ZK, *J Mole Cat B: Enzym* **56(4)**:189–195 (2009).
- [28] Nune M, Krishnan UM and Sethuraman S, *Mater Sci Eng C* **62**: 329–337 (2016).
- [29] Ignatova M, Manolova N and Rashkov I, *Eur Polym J* **43(5)**: 1609–1623 (2007).
- [30] Ross S, Topham PD and Tighe BJ, *Polym Int* **63(1)**: 44-51 (2014).
- [31] Fang R, Zhang E, Xu L and Wei S, *J Nanosci Nanotechnol* **10(11)**: 7747-7751 (2010).
- [32] Eda G and Shivkumar S, *J Appl Polym Sci* **106(1)**: 475–487 (2007).
- [33] Vaz CM, van Tuijl S, Bouten CVC and Baaijens FPT, *Acta Biomater* **1(5)**: 575–582 (2005).
- [34] Buschle-Diller G, Cooper J, Xie Z, Wu Y, Waldrup J and Ren X, *Cellulose* **14(6)**: 553–562 (2007).
- [35] Boland ED, Pawlowski KJ, Barnes CP, Simpson DG, Wnek GE and Bowlin GL, Electrospinning of bioresorbable polymers for tissue engineering scaffolds, in *Polymeric Nanofibers*, ed. by Reneker DH and Fong H, American Chemical Society, USA, vol. **918**, pp. 188-204 (2006).
- [36] Coleman MM, Graf JF and Painter PC, A practical guide to polymer miscibility, in *Specific Interactions and the Miscibility of Polymer Blends*, ed. by Coleman MM, Graf JF and Painter PC, Technomic, Lancaster, PA, pp. 49-153 (1991).
- [37] Ross S, Mahasaranon S and Ross GM, *J Appl Polym Sci* **132(14)**: 1-8 (2015).
- [38] Yooyod M, Ross GM, Limpeanchob N, Suphrom N, Mahasaranon S and Ross S, *Eur Polym J* **81**: 43–52 (2016).
- [39] Wang L, Topham PD, Mykhaylyk OO, Yu H, Ryan AJ, Fairclough JPA and Bras W, *Macromol Rapid Commun* **36(15)**: 1437-1443 (2015).
- [40] Li Z and Wang C, Effects of Working Parameters on Electrospinning, in *One-Dimensional nanostructures Electrospinning Technique and Unique Nanofibers*, ed. by Li Z and Wang C, Springer, New York, USA, pp. 15-28 (2013).
- [41] De Vrieze S, Van Camp T, Nelvig A, Hagström B, Westbroek P and De Clerck K, *J Mater Sci* **44(5)**: 1357–1362 (2009).
- [42] Fong H, Chun I and Reneker DH, *Polymer*, **40(16)**: 4585–4592 (1999).
- [43] Yu JH, Fridrikh SV and Rutledge GC, *Polymer* **47(13)**: 4789–4797 (2006).
- [44] Agarwal S, Wendorff JH and Greiner A, *Polymer* **49(26)**: 5603–5621 (2008).
- [45] Ross S, Mahasaranon S and Ross GM, *Macromol Symp*, **354(1)**: 76–83 (2015).